Available online at www.sciencedirect.com
SCIENCE DIRECT
International Journal of Heat and Mass Transfer 49 (2006) 2535–2544
International Journal of HEAT and MASS TRANSFER
www.elsevier.com/locate/ijhmt

An experimental study of heater size effect on micro bubble generation

Peigang Deng [a], Yi-Kuen Lee [a,*], Ping Cheng [b]

[a] Department of Mechanical Engineering, The Hong Kong University of Science and Technology, Hong Kong SAR, China
[b] School of Mechanical and Power Engineering, Shanghai Jiaotong University, Shanghai 200030, China

Received 14 July 2005; received in revised form 29 September 2005
Available online 20 March 2006

Abstract

An experimental study of the heater size effect on micro boiling is reported in detail. Using a 1.66-ms-wide heating pulse, boiling in subcooled water was investigated on a series of micron/submicron thin film Pt heaters with various feature sizes ranging from 0.5 μm to 70 μm. It was found that there existed a critical heater size (10 μm): single spherical bubble generation with heater's feature size less than 10 μm; oblate vapor blanket on the heater surface with the size larger than 10 μm. The bubble dynamics was studied by the visualization of the bubble nucleation process with a high-speed CCD. The onset bubble nucleation temperature was measured by using each Pt heater as a resistive temperature sensor. The formation of the oblate vapor blanket was attributed to the condensation effect of the vapor outside the superheated zone. The analysis was further validated by generating spherical bubble on heater with size larger than 10 μm with a longer heating pulse.

Keywords: Size effect; Micro heater; Micro boiling; Micro bubble actuator

1. Introduction

Microscale boiling and transient bubble nucleation phenomena have been investigated extensively in recent years. The advancing MEMS technology enables the fabrication of heaters with sizes down to microns or even submicrons, which can result in a much higher heat flux from the heater surface. It is well known that cavities on the heater surface can be an important factor for the bubble nucleation in both pool boiling and flow boiling. Based on MEMS technology, heaters can be fabricated with surfaces totally free of noticeable cavities or, on the contrary, with artificial cavities created by wet etching or dry etching, cavities with well-defined sizes and shapes. These unique characteristics of micro heaters, together with the advanced experimental apparatus, such as an optical microscope and a high-speed CCD camera, have aroused great interest in investigating the differences in the mechanisms between the conventional macroscale and microscale boiling and bubble nucleation.

Prior to the now widely-used IC-processed planar heater, thin metal wires had been extensively employed for transient boiling study. Using a very thin platinum wire, Skripov et al. [1] experimentally investigated spontaneous bubble nucleation in water and organic liquids. Analysis of experimental data on nucleation kinetics and verification of the homogeneous nucleation theory were conducted. Similar studies were carried out by Derewnicki [2] in water, Okuyama and Iida [3] in liquefied nitrogen and Okuyama et al. [4] in Refrigerant R-113. A heating rate in the order of 10^6–10^7 K/s was imposed in these studies.

Lin et al. [5,6] investigated the bubble formation mechanism on a polysilicon micro resistor both in an open environment and in micro channels. Individual spherical vapor bubbles were generated on the micro heater and a strong Marangoni effect was observed. It was also found that the cavity theories for pool boiling experiment (macro boiling) are not generally applicable to micro boiling due to the cavity size being 10.7 nm (via Atomic Force Microscope

* Corresponding author. Tel.: +852 2358 8663; fax: +852 2358 1543.
E-mail address: meyklee@ust.hk (Y.-K. Lee).

0017-9310/$ - see front matter © 2006 Elsevier Ltd. All rights reserved.
doi:10.1016/j.ijheatmasstransfer.2005.12.016

surface analysis) and higher superheat close to the superheat limit.

Iida et al. [7] investigated the bubble nucleation in ethyl alcohol, toluene and water using a small Pt/Cr film heater ($100 \times 250\ \mu m^2$) sputtered on a quartz glass substrate and at an extremely high heating rate of about 10^8 K/s. It was observed that a large number of tiny bubbles of almost uniform diameter generated concurrently on the heater, and the incipient bubble nucleation temperature increased with the rate of temperature rise and reached a saturated value at a certain high rate. In another study, Okuyama et al. [8] used the same experimental apparatus as Iida et al. [7] to investigate the transient boiling in ethyl alcohol at a heating rate of 10^7 K/s, where special emphasis was placed on the boiling dynamics and the corresponding heat transfer from the heater surface. The concurrently generated tiny bubbles coalesced to form a large bubble slightly after the boiling incipience and the heat flux decreased to about half of the value before boiling. It was deduced that the energy stored in the superheated liquid layer adjacent to the heater surface dominated the growth and collapse of the coalesced bubble.

Avedisian et al. [9] measured the bubble nucleation temperature on a Ta/Al heater of a commercial thermal ink-jet printer (TIJ) under various heating rates. The bubble nucleation temperature increased with the heating rate and approached a maximum value of 560 K, which corresponds to a maximum heating rate of 2.5×10^8 K/s. It was pointed out that the high heating rate associated with ink-jet printing was a special case where homogeneous nucleation at a smooth solid surface can occur before nucleation boiling on the rough part of the surface. Oh et al. [10] established a vapor bubble formation model based on molecular interactions, and an expression of the bubble nucleation rate was given. From a 3-D heat conduction numerical simulation, it was revealed that bubble formation on the heater is possible when the maximum temperature point of the heater was greater than the superheat limit of the liquid by 6–12°C.

Zhao et al. [11] and Glod et al. [12] measured the acoustic pressure waves as the bubbles formed on a $100 \times 110\ \mu m^2$ thin film and a platinum wire with of 10 μm in diameter, respectively. It was found that the acoustic pressure emission increased linearly with time shortly after the onset of explosive vaporization. The extractable mechanical power for explosively expanding vapor bubbles was estimated to be about 0.5 W.

Kim et al. [13] studied subcooled pool boiling on a small heater array ($0.27 \times 0.27\ mm^2$) in low, earth and high gravity environments; Tsai and Lin [14] studied bubble formation on polysilicon micro resisters ($95 \times 10\ \mu m^2$, $95 \times 5\ \mu m^2$); Jung et al. [15] investigated bubble nucleation on micro line heaters ($50 \times 3\ \mu m^2$, $50 \times 5\ \mu m^2$) under steady or finite pulse of voltage input; Yin et al. [16] studied the bubble nucleation on an impulsively powered micro heater ($260 \times 260\ \mu m^2$) at different heat fluxes between 3 and 44 MW/m^2. An overall picture of the recent research work on micro boiling can be found in two review papers given by Lin [6] and Yang [17], respectively.

Various shapes of vapor bubbles have been reported in the study of microscale boiling and transient bubble nucleation in recent years. For example, micro spherical bubbles were reported by Lin [6], Tsai [14] and Jung [15]; an oblate vapor blanket was observed by Zhao [11] and Yin [16]; coalescence of tiny bubbles into a large vapor blanket was observed by Okuyama [4], Iida [7] and Hong [18]. Early in 1966, the shape of the bubble in nucleate boiling was investigated by Johnson et al. [19] and the differences in bubble shapes, hemispherical or spherical bubble, were explained on the basis of the relative importance of the inertial force and surface tension force. Recently, the shape of the vapor/liquid interface in nucleation boiling was investigated by Lay [20] and Chen [21]. Various forces acting on the interface were analyzed to determine the bubble shape, which may include buoyancy force, contact pressure force, surface tension force, inertia force, drag force, etc.

In our previous studies, we have investigated micro bubble generation on non-uniform-width micron/submicron heaters ($10 \times 3\ \mu m^2$, $0.5 \times 0.5\ \mu m^2$) under pulse heating [22–24], the transient micro thermal bubble generation and its subsequent dynamic behavior in single-stranded DNA solutions [25–27]. The observation of the single spherical bubble generation on the micron/submicron heaters aroused our research interest in revealing the heater size effects on boiling patterns. Generally speaking, in addition to the working liquid itself, two factors can distinctly affect the boiling patterns: the characteristics of the micro heater itself and the way in which the electric power is imposed on the heater. The former may include different sizes of the heater, the material and the surface properties of the heater. The latter may include continuous heating or transient heating, the transient heating pulse width, and the power input to the heater. The heating power and the size of the heater determine the amount of heat flux from the heater. Although much research on micro boiling has been conducted on several different sizes of the micro heaters, as introduced before, the material and the fabrication of the heaters and also the heating methods were usually not the same. Therefore, it is worthwhile to investigate the heater size effects on the microscale boiling and bubble nucleation process, while the material and the micro fabrication process of the heaters should be the same and a consistent heating criterion should be used.

In this paper, we will report our study on transient water boiling on a series of thin film planar Pt heaters, simultaneously fabricated on the same silicon wafer and with various feature sizes ranging from 0.5 μm to 70 μm. Note that the "micro boiling" in the present paper refers to bubble nucleation on micro heaters. A 1.66-ms-wide voltage pulse was imposed on each Pt heater, while the height of the voltage pulse was increased from zero until boiling was observed at a certain voltage. Thus, the power input to the heater was the minimum one required to induce a boiling process, which is called "onset boiling" in the present paper. Note that 1.66 ms is an optimum working heating

pulse for our micro bubble actuator [25–27], and the bubble nucleation under other heating pulse widths has been investigated in our previous study [22]. The bubble nucleation process was visualized by a high-speed CCD camera (PCI 8000s, MotionScope Inc.). The onset bubble nucleation temperature was measured by using each Pt heater as a self-sensing resistive temperature sensor, and a 100 MHz high-speed digitizer (NI 5112, National Instruments) was used for data acquisition.

2. Design and fabrication of the micron and submicron Pt heaters

Fig. 1 shows the pictures of the packaged heater chips and some typical micron/submicron heaters. Note that there were no noticeable cavities on the surfaces of the heaters. All the Pt heaters adopted the non-uniform-width design to restrict the high temperature area just at the slim part of the heater [22]. The dimensions of the heaters are listed in Table 1, and the width of the slim part of the heater was regarded as the feature size of the heater, which ranged from 0.5 μm to 70 μm.

The fabrication of the heaters with a 4-inch Si wafer started with a 500 nm thermal oxidation and 1500 nm LPCVD silicon nitride as the thermal isolating layer. Submicron and micron photolithography were realized with projection printing (ASML Stepper 5000) and contact aligner (Karl Suss MA6), respectively. A 10 nm Ti layer and 150 nm Pt layer were then sputtered and lift-off for the submicron Pt heater. After the sputtering process, the sheet resistance of the Pt film was measured to be 1.64 Ω/sq. Similarly, 10 nm TiW layer and 200 nm Au layer were also sputtered and lift-off for the electric pad. After the micro fabrication and wafer dicing, the micron and submicron heater chip were mounted separately on a printed circuit board (PCB), and the electric pads on the chip were wire bonded to the PCB (Fig. 1).

Table 1
Dimensions of some of the micron/submicron heaters

	Heater ID	Length (μm, ±2%)	Width (μm, ±3%)
Submicron heater	(a)	0.5	0.5
	(b)	1	0.5
Micron heater	(c)	2	1
	(d)	10	3
	(e)	10	5
	(f)	20	10
	(g)	30	10
	(h)	30	15
	(i)	90	30
	(j)	150	50
	(k)	200	70

The length and width are those of the slim part of the heater (refer to Fig. 1).

3. Experimental setup

In this experiment, the heaters were operated under pulse heating conditions. A schematic diagram of the experimental setup is shown in Fig. 2(A), and the control circuit for the heating pulse generator is shown in Fig. 2(B). A programmable 8255 I/O card was used to generate a pulse train, which was sent to the base terminal of a high gain transistor (ZTX689B, Zetex) to control the on/off heating process. The pulse generated from an 8255I/O card was also sent to a CCD camera (PCI 8000s MotionScope Inc.) and a 100 MHz high-speed digitizer (NI 5112, National Instruments) to trigger the video recording and the voltage recording (V_T in Fig. 2(B)) during the pulse heating period. By employing the Pt heater as a resistive temperature sensor, the average temperature variation of

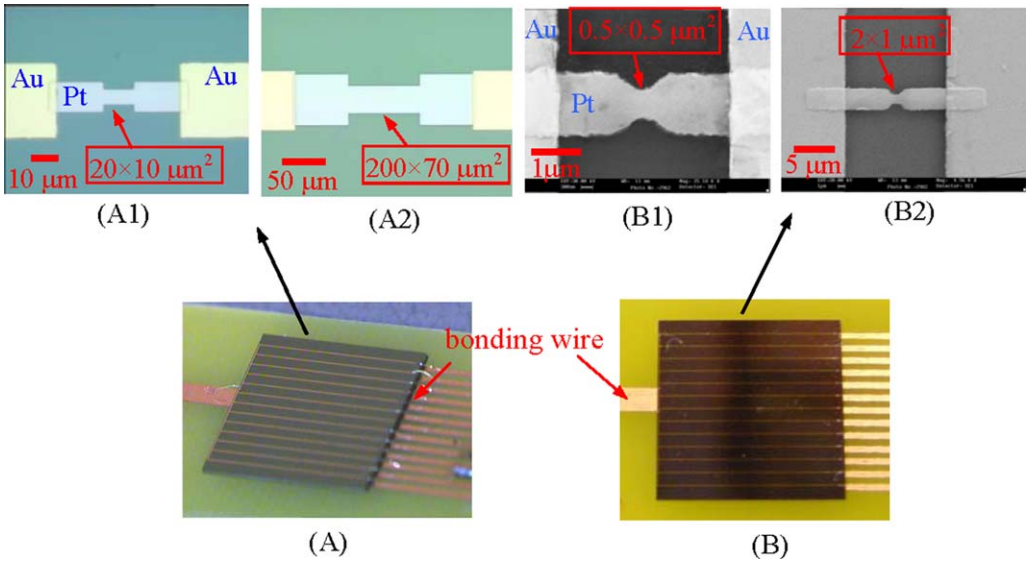

Fig. 1. Packaged chips of (A) micron heaters and (B) submicron heaters, and pictures of the non-uniform-width micron/submicron Pt heaters: (A1), (A2) optical micrographs of the micro heaters; (B1), (B2) SEM pictures of submicron heaters.

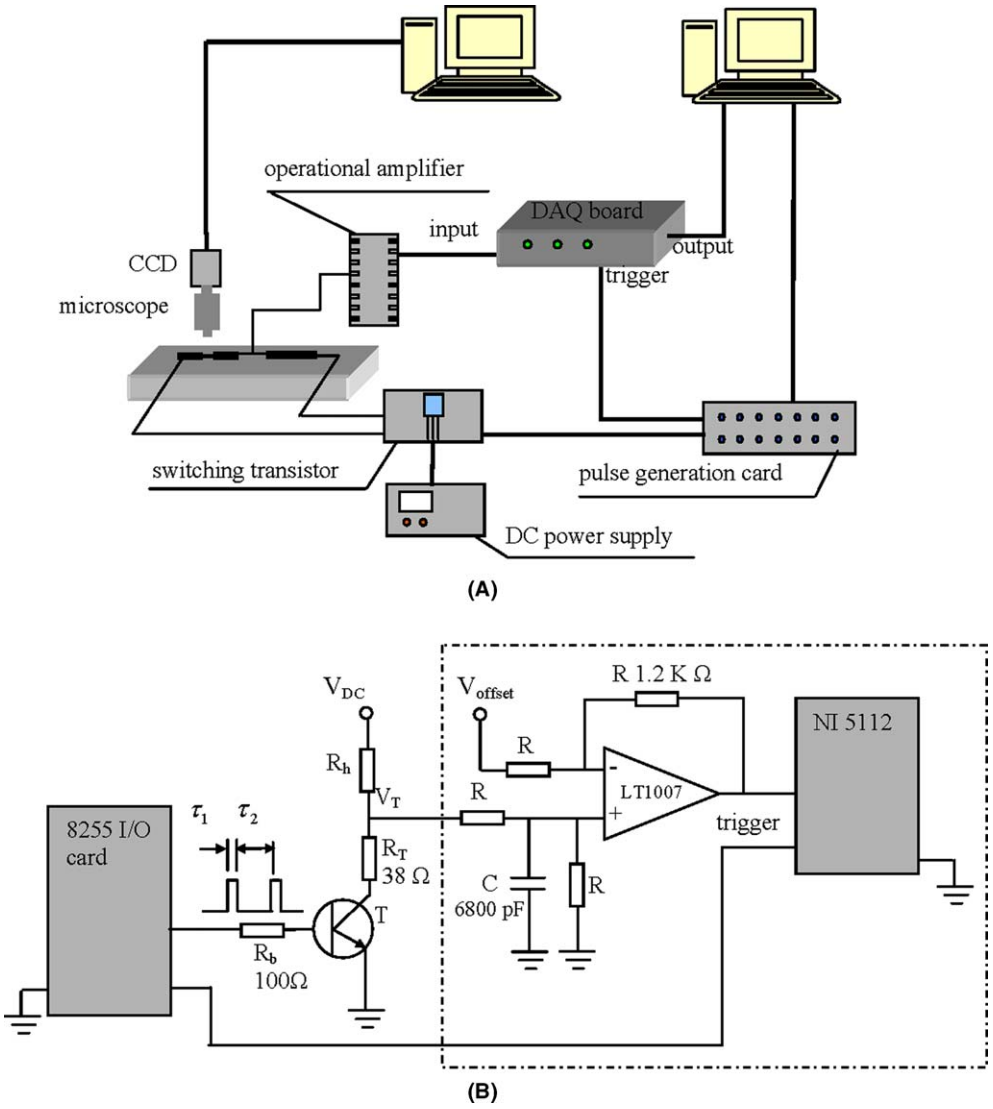

Fig. 2. (A) Schematic diagram of experimental set-up and (B) control circuit of the micro heater.

the heater during the pulse-heating period was measured, which could be used to evaluate the bubble nucleation temperature. A detailed description of the temperature measurement method as well as the error analysis was given in [26]. A DC power supply (model DF1731SB, Gold-source Inc.), which controlled the magnitude of the heating pulse in the micro heater, was connected to the collector terminal of the transistor and the emitter terminal was grounded. The pulse width, τ_1 in Fig. 2(B), varied from several microseconds to milliseconds, and a typical heating pulse width 1.66 ms was used in the present experiment. To avoid the overlapping of bubbles, a waiting pause τ_2 of 1 s was inserted between two consecutive heating pulses.

4. Results and discussion

4.1. Heater size effects on boiling patterns

To make a fair comparison of the heater size effects on micro boiling, a consistent heating criterion should be taken in addition to the same material and the same fabrication process. We investigated the "onset" boiling on each heater in the present study to reveal the heater size effects on boiling patterns. Under a 1.66-ms heating pulse, the onset boiling phenomena on the micron/submicron Pt heaters were investigated in water, which was loaded onto the heater chip by a pipette and contacted the micro heater directly. The water was at 298 K (room temperature) and its volume was much larger than the size of the heater. From the video taken during the transient boiling on the heaters, it was found that there existed a critical feature size of the heater, 10 μm in this case. The boiling patterns on heaters with feature size below or above this critical value were quite different, and they were classified into two groups:

Group I (heaters (a)–(f)): single spherical bubble generation with heaters' feature size less than or equal to 10 μm;

Group II (heaters (g)–(k)): oblate vapor blanket on the heater surface with heaters' feature size larger than 10 μm.

4.1.1. Boiling patterns of Group I

A series of typical snapshots of the boiling pattern of Group I, taken from submicron heater (b) and micron heater (e), are shown in Fig. 3, in which the power input and the heat flux from the heater surface were also indicated. Note that the power input was calculated on the basis of the resistance of the micro heater at room temperature [25], and it could change as the resistance increased with temperature during the pulse-heating period. The heat flux was the rate of heat generation from the heater surface.

For Group I, a spherical bubble was generated precisely on the slim part of the non-uniform-width heater, and it grew rapidly until reaching its maximum size at the end of the 1.66-ms heating pulse. After that, the bubble gradually collapsed on the heater surface. In order to characterize single bubble dynamics quantitatively, the bubble diameter in each frame of the digitalized videos was measured using a Matlab program. The bubble diameter as a function of time covering the entire bubble generation and collapse process is presented in Fig. 4. The error of the present bubble size measurement method stemmed mainly from the difficulty of identifying the borderline of the bubble geometry accurately. Based on repeated measurements for the same bubble picture, an absolute error of ± 0.2 μm was found for measurements on submicron heaters (a), (b) and micro heaters (c), (d); and ± 0.5 μm for measurements on micro heaters (e). As shown in Fig. 4, the profiles of the bubble diameter–time curves (from I–V) are very similar to each other and a clear bubble growth and collapse process was recorded. Generally, the maximum bubble diameter was comparable to the size of the micro heater due to the highly localized boiling. The bubble growth period on each heater was comparable to the width of the heating pulse (1.66 ms). After reaching its maximum size, the bubble began to collapse on the heater surface, which was longer than the growth period and could last 10–450 ms. Generally, both the maximum bubble diameter and bubble lifetime decreased with the heater size due to the shrunk superheated zone in water. No bubble departure was observed in the repeated tests in this experiment, which was attributed to the highly localized boiling mechanism for the present case.

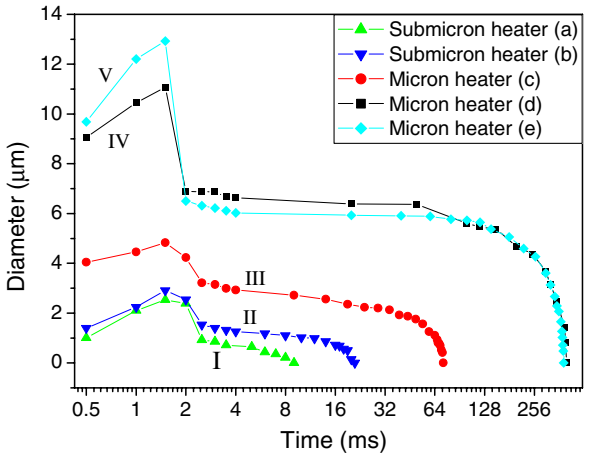

Fig. 4. Semi-logarithmic plot of the bubble diameter versus time for the boiling process of Group I. Curves I and II: bubble nucleation on submicron heater (a) and (b); Curves III, IV and V: bubble nucleation on micron heater (c), (d) and (e).

The classical bubble dynamics simply divide the bubble growth process into two stages: an isothermal process at the initial stage and a subsequent isobaric process [28]. For the isothermal process, corresponding to the inertial-controlled bubble growth, the bubble growth is driven by the pressure difference between the vapor phase and the liquid phase at the bubble interface. The bubble diameter as a function of time can then be expressed as $D = D_0 t$ for $D \gg D_i$, where D_0 is a constant and D_i is the initial bubble diameter, which can be as small as 1–10 nm [29]. For the isobaric process, corresponding to the thermally-controlled bubble growth, the bubble growth is governed by the rate at which heat can be supplied from the superheated liquid layer to the bubble interface to facilitate the vaporization process. The variation of bubble diameter with time can be expressed as $D = D_{0t} t^{1/2}$, where D_{0t} is a constant.

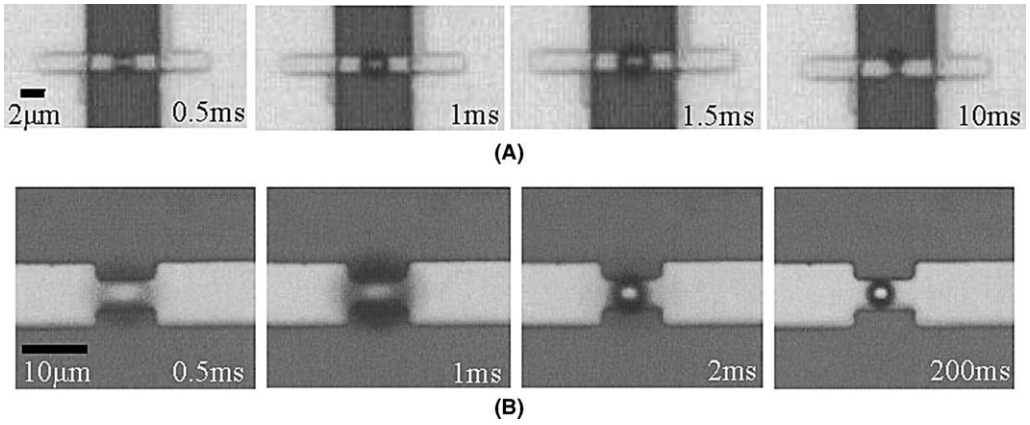

Fig. 3. Boiling pattern of Group I: single spherical bubble generation in water under 1.66-ms pulse heating. (A) On submicron heater (b), pulse heating power: 1.3 mW, heat flux 112.4 MW/m^2. (B) On micron heater (e), pulse heating power: 38.5 mW, heat flux 85.2 MW/m^2.

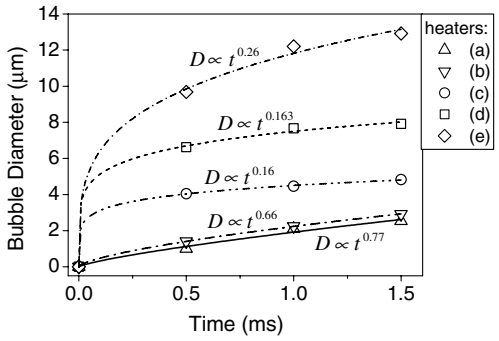

Fig. 5. Comparison of the bubble growth curve on different heaters.

In Fig. 5, the bubble growth curves on various heaters were fitted with a form of $D = D^* t^b$, where D^* and b are constant. Obviously, for an isothermal bubble growth b is equal to 1, and for isobaric bubble growth b is equal to 0.5. It was found that for the bubble generation on submicron heaters, the value of b was between 0.5 (thermally-controlled bubble growth) and 1 (inertial-controlled bubble growth); while for that on micron heaters, the value of b was lower than 0.5.

4.1.2. Boiling patterns of Group II

Fig. 6 shows the typical snapshots of the boiling pattern of Group II, taken from micron heaters (j) and (l), which were quite different from those of Group I, as shown in Fig. 3. No single spherical bubble was observed, and instead, an oblate vapor blanket formed on the heater surface and it disappeared almost immediately after the pulse heating stopped at 1.66 ms. During the vapor condensation process, some small bubbles may form on the heater surface. From all the snapshots of the Group I and II, it was found that the light intensity of the vapor layer on the surfaces of heaters of Group II was fairly uniform (Fig. 6), indicating a relatively planar vapor/liquid interface. However, on the surfaces of heaters of Group I, the light intensity of the vapor layer was much brighter at the middle of the bubble (Fig. 3), indicating a much curved (spherical) vapor/liquid interface.

4.1.3. Transition of the boiling patterns of Groups I and II

Boiling patterns on heaters with feature size of 10 μm was a transition from Group I to II. As shown in Fig. 7(A), the boiling pattern on heater (f) (20×10 μm^2) actually was very similar to that of Group I. An ellipsoidal bubble was generated on the slim part of the heater with the arrival of the heating pulse, and the bubble growth process was also restricted within the slim part of the micro heater. It began to collapse on the heater surface at the end of the 1.66-ms heating pulse, which was a slow process and lasted for 130 ms. However, the boiling pattern on heater (g) (30×10 μm^2) was similar to that of Group II as shown in Fig. 7(B). An elongated ellipsoid vapor layer was observed on the heater surface during the pulse heating period, and it disappeared sooner after the heating pulse stopped. The experimental observation on heaters (f) and (g) implied that as the heater size was increased in its planar dimension, the boiling patterns changed from Group I to Group II.

In summary, Fig. 8 shows the map of boiling pattern with respect to the heater size from the boiling experiments on all the heaters. The critical feature size of the heater 10 μm was clearly shown for the present transient boiling.

4.2. Onset bubble nucleation temperatures

Fig. 9 shows the measured average temperature variation of the heaters with respect to time for the onset bubble nucleation in water on submicron heaters (a), (b) and micron heaters (c), (d), (f) and (i). Since the bubble gener-

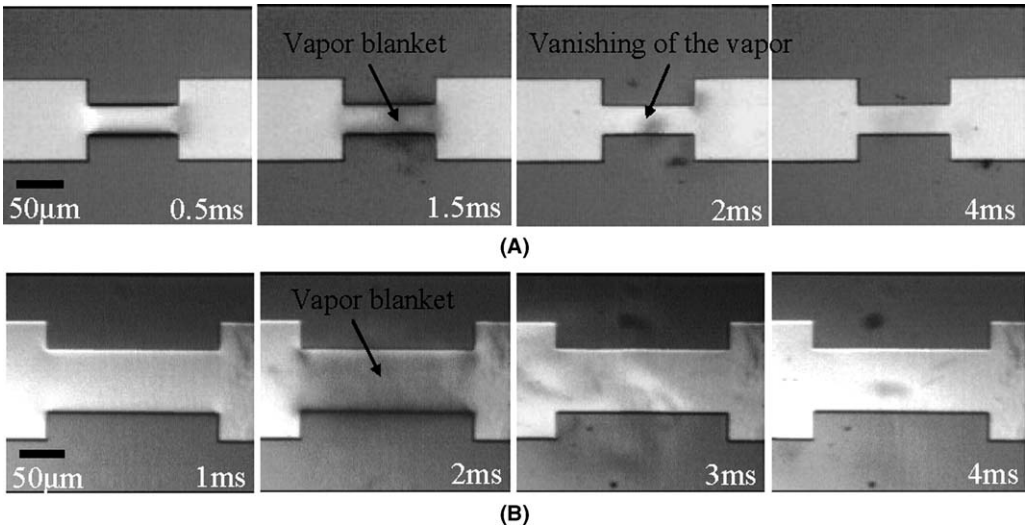

Fig. 6. Boiling pattern of Group II: oblate vapor blanket on the heater surface. (A) on micron heater (i) pulse heating power 808.2 mW, heat flux 46.3 MW/m^2 (B) on micron heater (k), pulse heating power 5565 mW, heat flux 114.6 MW/m^2.

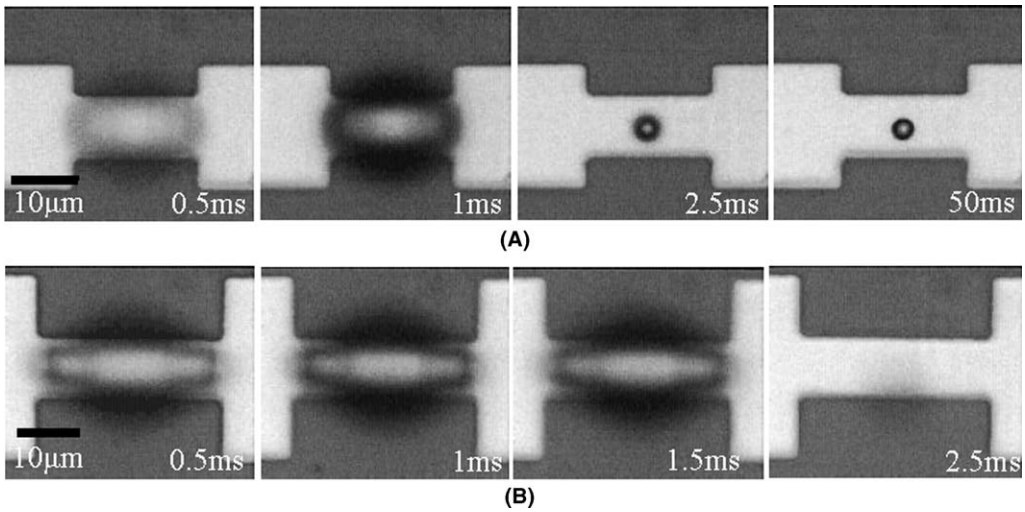

Fig. 7. Transition region of the boiling pattern on heaters with feature size 10 μm. (A) boiling on heater (f), pattern of Group I, pulse heating power 100.1 mW, heat flux 76.2 MW/m^2, (B) boiling on heater (g), pattern of Group II, pulse heating power: 141.9 mW, heat flux 46.4 mW.

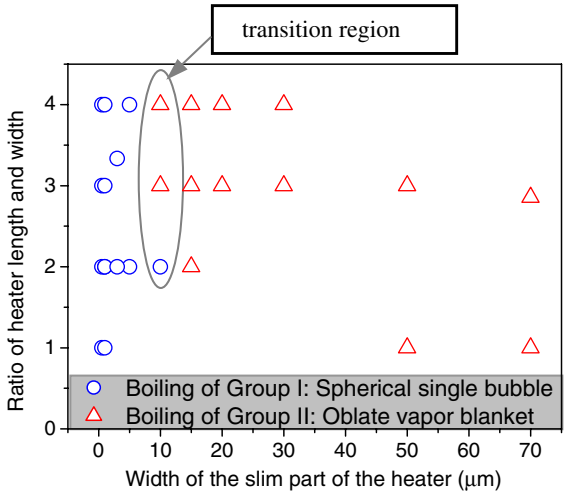

Fig. 8. Map of boiling patterns on micro heaters of various sizes.

ation process was very stable and repeatable, there was no noticeable change of the temperature–time curve during the repeated pulses. As shown in Fig. 9, at the initial stage after the beginning of the pulse heating, the average temperature of the heater increased exponentially with time for all the heaters, indicating a lumped capacitance heat conduction characteristics. The heating rate at this stage was in the range of 10^6–10^7 K/s, and the high heating rate was observed on submicron heaters due to their low thermal capacity. Note that this heating rate was similar to the experiment performed by Skripov [1], who showed that a heating rate as high as 6×10^6 K/s was required for homogeneous nucleation around a platinum heating wire.

In curves I, II and III of Fig. 9, a temperature inflection point was observed on submicron heaters (a), (b) and micron heater (c), after the initial exponential increase of the heater temperature. A close-up view of the temperature inflection was shown in insert A. The temperature inflection point has been observed by other researchers in their study on transient micro boiling and the temperature at the inflection point was regarded as the bubble nucleation temperature [9,12]. Thus, according to the inflection points in curves I, II and III of Fig. 9, the bubble nucleation temperature on heaters (a), (b) and (c) was 518 K, 480 K and 487 K, respectively. The corresponding bubble nucleation time (the time of the occurrence of bubble nucleation after the beginning of the heating pulse) was 51 μs, 60 μs and 72 μs on heaters (a), (b) and (c), respectively. It was also found that, after the incipience of bubble nucleation, the average temperature of the heaters (a), (b) and (c) still increased distinctly till the end of the heating pulse.

For bubble nucleation on micron heaters (d), (f) and (i), however, the temperature inflection point was not observed. Instead, the temperature increase curves (IV, V and VI) experienced a "V" shape change, as indicated in Fig. 9: they suddenly dropped for 10–20 K and after that slowly increased until the end of the heating pulse. The "V" shape temperature change was also observed and speculated as an indication of the beginning of bubble nucleation in our previous study on bubble nucleation temperature in DNA solutions, in which the bubble was generated on a micron heater (10×2 μm^2) with parylene coating [26]. So, according to curves IV, V and VI in Fig. 9, the bubble nucleation temperature on heaters (d), (f) and (i) was 485 K, 478 K and 473 K, respectively, and the corresponding bubble nucleation time was 240 μs, 236 μs and 324 μs.

4.3. Power input and heat flux for the onset bubble nucleation

Fig. 10 is a plot of the power input to each heater and the corresponding heat flux from the heater surface for all the cases of onset boiling on submicron heaters (a), (b) and micron heaters (c)–(k). It is found that the power input to the heater increases with the feature size of the

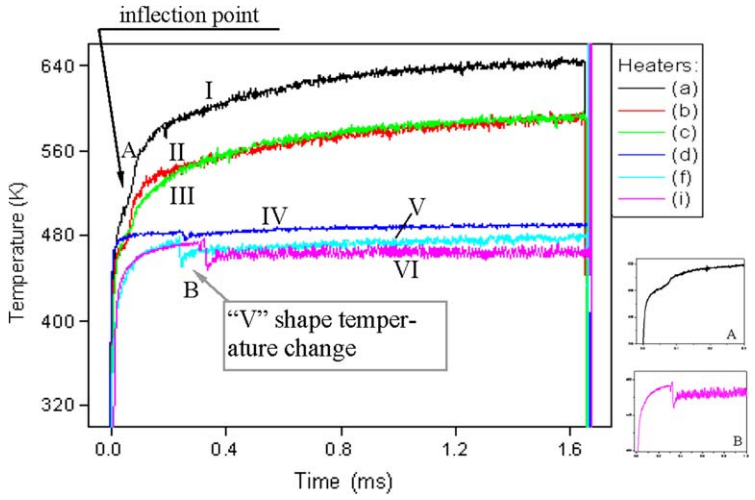

Fig. 9. Measured average temperature of the heaters as a function of time for onset bubble nucleation in water. Refer to Fig. 10 for the power input and heat flux.

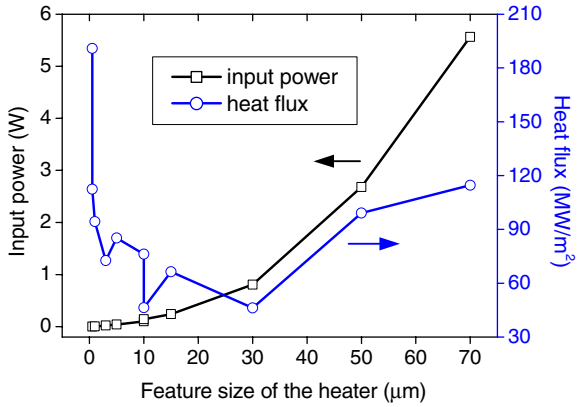

Fig. 10. Heater size effects on power input to each heater for the onset of bubble nucleation and the corresponding heat flux from the heater surface.

heater: for the boiling on heater with feature size less than 1 μm, the power input was just several milli-watts; for that on heater with feature size in between 1 μm and 10 μm, the power input was less than 100 mW; for that on heater with feature size larger than 10 μm, the power input increased very fast and could be larger than 1 W. Since the superheated zone in water was comparable to the size of the heater, more water was heated up to a high temperature on larger heaters and therefore a larger power input was required for the onset boiling on larger heaters.

Fig. 10 also shows a "U" shape curve of the variation of the heat flux with respect to the increase of the heater size shows. It is known that the heat flux is determined by the power input to the heater and the area of the heater. For the onset boiling on heaters with the feature size less than 10 μm, the heat flux decreased with the increase of the heater size, although the power input increased. Thus, in these cases, the increase of the heater area dominated the heat flux on the heater surface. The situation was reversed as the feature size of the heater was larger than 10 μm, where the heat flux increased with the feature size of the heater. In these cases, the power input showed a notable increase and it dominated the heat flux on the heater surface, although the area of the heater also increased.

4.4. Discussions on boiling patterns

The present transient boiling on micro heaters emerged in the subcooled water was a highly localized boiling process, which means a quite large temperature gradient existed in the water near the heater surface. Actually, a 3D heat conduction model revealed that for the onset boiling under 1.66-ms heating pulse the superheated zone in the liquid was $12 \times 3 \times 4\ \mu m^3$ on a $10 \times 3\ \mu m^2$ micro Pt heater [22]. The growth of the vapor will be mainly restricted within the superheated zone of the water because of the condensation effect outside the superheated region.

After the incipience of boiling, the water–vapor interface would try to shrink to a spherical shape due to the existence of surface tension, which is the dominant force at the microscale level. Consequently, the vapor would shrink from its sides and accumulate to form a spherical vapor volume. This attempt eventually resulted in the spherical bubble formation on heaters with feature size less than 10 μm, however the spherical bubble was not formed on heaters with feature size larger than 10 μm. The reason might be that a relatively larger bubble on a larger heater will go beyond the very thin superheated zone. As a result, the upper part of the vapor bubble will be condensed, and the vapor will looks like a vapor blanket.

To verify our explanation of the heater size effects on micro boiling patterns, boiling on heaters of Group II with longer heating pulse was investigated. A longer heating pulse will increase the thermal diffusion depth and produce a thicker superheated zone in water, and thus spherical bubble might be observed within this thicker superheated zone on heaters with feature size larger than 10 μm.

Two heaters: micro heater (i) and (j) were selected for the testing and for each heater, the imposed voltage (V_{DC} in Fig. 2(B)) was fixed at the value for onset boiling under the 1.66-ms-wide heating pulse. The heating pulse width was gradually increased starting from 1.66 ms and the boiling process was recorded by a CCD camera (TK-C1381, JVC Co.) with a conventional recording speed (25 fps). As shown in Fig. 11, single spherical bubble could be formed on micron heater (i) with a heating pulse width of 150 ms, and on micron heater (j) with a heating pulse width of 336 ms. Similar to that of boiling Group I, the micro bubble was nucleated on the slim part of the heater, and the bubble size comparable to the size of the slim part of the heater. For bubble generation on heater (i), the bubble expanded during the pulse heating period. A maximum bubble diameter of about 60 μm was recorded at near the end of the heating pulse and after that the bubble gradually collapsed on the heater surface. The bubble collapse was a much longer process, which lasted for 252 s on heater (i). This is quite different from the bubble collapse of boiling Group I (with heating pulse 1.66 ms), in which the bubble collapse process was no longer than 450 ms. It seems that there was still incondensable gas dissolved in the testing water, although it has been degassed by boiling on a hotplate for 3 h before use. To explain the much longer bubble collapse as shown in Fig. 11(A), the mass diffusion of the incondensable gas inside the bubble might be considered [30] and it is beyond the scope of this paper. For bubble generation on heater (j), the bubble expanded during the pulse-heating period and then departed from the heater surface at a diameter of about 250 μm sooner after the heating pulse stopped. The detachment of the bubble could be mainly attributed to two reasons. The first one is the inertia effect due to a relatively long vapor expansion process—336 ms on heater (j), compared to that of 150 ms on heater (i). The second one is the buoyancy force, which was approximately 2 order-of-magnitude larger for the bubble on heater (j) (250 μm) than that for the bubble on heater (i) (60 μm).

5. Concluding remarks

To investigate heater size effects on micro boiling, transient (1.66 ms-width pulse heating) onset boiling in subcooled water was studied on a series of micron/submicron thin film Pt heaters, which had various feature sizes ranging from 0.5 μm up to 70 μm. It was found that the size effect of the heater could dramatically affect the boiling pattern, and they were classified into two groups. Group I: single spherical bubble generation with heater's feature size less than 10 μm; Group II: oblate vapor blanket on the heater surface with heater's feature size larger than 10 μm. For boiling of Group I, the size of the micro single bubble was comparable to the size of the heater, as well as that of the superheated zone in the fluid. The bubble growth period was comparable to the width of the heating pulse, and the bubble collapsed on the heater surface without detachment.

Onset boiling temperature was measured by using the heaters as a resistive temperature sensor. The heating rate at the initial stage after heating was in the range of 10^6–10^7 K/s. The highest nucleation temperature 518 K was observed on submicron heater (a), corresponding to a superheat of 145 K. For boiling on other heaters, the nucleation temperature was around 480 K, corresponding to a superheat of 107 K. As to the bubble nucleation time, it increased with the size of the heater.

The heater size effect could also affect the power input and heat flux for the onset of boiling. The power input to the heater showed an exponentially increase with the feature size of the heater: it increased slowly with the size on small heaters, while increased rapidly on large ones. The variation of the heat flux with respect to the increase of the heater size shows a "U" shape curve. For boiling on

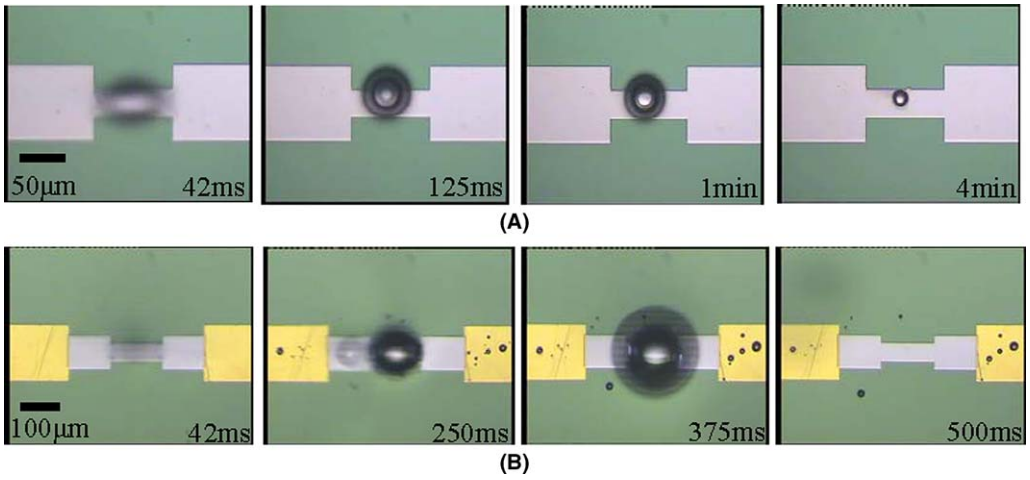

Fig. 11. Spherical single bubble generation on micro heater (i) and (j): (A) heater (i): heating pulse 150 ms, heating power 808.2 mW, heat flux 46.3 MW/m^2; (B) heater (j): heating pulse width 336 ms, heating power 2681 mW, heat flux 99.1 MW/m^2.

heaters with feature size less than 10 μm, the heat flux decreased with the increase of the heater size, while it increased with the size for boiling on heaters with feature size larger than 10 μm.

The formation of the oblate vapor blanket of boiling Group II was attributed to the condensation effect of the vapor outside the superheated zone in water. The analysis was further validated by generating spherical bubble on heater with size larger than 10 μm with a longer heating pulse. More detailed numerical simulation of the bubble dynamics has been in progress to achieve better prediction of the critical heater size.

Acknowledgements

This work was supported by the Hong Kong Research Grant Council (HKUST6134/04E). The third author would like to acknowledge the partial support of this work by Natural National Science Foundation of China through Grant #50536010.

References

[1] V.P. Skripov, Metastable Liquids, John Wiley, New York, 1974 (Chapters 4 and 6).
[2] K.P. Derewnicki, Experimental studies of heat transfer and vapor formation in fast transient boiling, Int. J. Heat Mass Transfer 28 (1985) 2085–2092.
[3] K. Okuyama, Y. Iida, Transient boiling heat transfer characteristics of nitrogen bubble behavior and heat transfer rate at stepwise heat generation, Int. J. Heat Mass Transfer 33 (1990) 2065–2071.
[4] K. Okuyama, Y. Kozawa, A. Inoue, S. Aoki, Transient boiling heat transfer characteristics of R113 at large stepwise power generation, Int. J. Heat Mass Transfer 31 (1988) 2161–2174.
[5] L. Lin, A.P. Pisano, V.P. Carey, Thermal bubble formation on polysilicon micro resistors, ASME J. Heat Transfer 120 (1998) 735–742.
[6] L. Lin, Microscale thermal bubble formation: thermophysical phenomena and applications, Microscale Thermophys. 2 (1998) 71–85.
[7] Y. Iida, K. Okuyama, K. Sakurain, Boiling nucleation on a very small film heater subjected to extremely rapid heating, Int. J. Heat Mass Transfer 37 (1994) 2771–2780.
[8] K. Okuyama, Y. Iida, Boiling bubble behavior and heat transfer succeeding spontaneous nucleation on a film heater, in: Proceedings of the 11th International Heat Transfer Conference (11th IHTC), Kyongju, Korea, 1998, pp. 23–28.
[9] C.T. Avedisian, W.S. Osborne, F.D. Mcleod, C.M. Curley, Measuring bubble nucleation temperature on the surface of a rapidly heated thermal ink-jet heater immersed in a pool of water, Proc. Roy. Soc. Lond. A 455 (1999) 3875–3899.
[10] S.D. Oh, S.S. Seung, H.Y. Kwak, A model of bubble nucleation on a micro heater, J. Heat Transfer 121 (1999) 220–225.
[11] Z. Zhao, S. Glod, D. Poulikakos, Pressure and power generation during explosive vaporization on a thin-film microheater, Int. J. Heat Mass Transfer 43 (2000) 281–296.
[12] S. Glod, D. Poulikakos, Z. Zhao, G. Yadigaroglu, An investigation of microscale explosive vaporization of water on an ultrathin Pt wire, Int. J. Heat Mass Transfer 45 (2002) 367–379.
[13] J. Kim, J.F. Benton, D. Wisniewski, Pool boiling heat transfer on small heaters: effect of gravity and subcooling, Int. J. Heat Mass Transfer 45 (2002) 3919–3932.
[14] J.H. Tsai, L. Lin, Transient thermal bubble formation on polysilicon microresistors, J. Heat Transfer 124 (2002) 375–382.
[15] J.Y. Jung, J.Y. Lee, H.C. Park, H.Y. Kwak, Bubble nucleation on micro line heaters under steady or finite pulse of voltage input, Int. J. Heat Mass Transfer 46 (2003) 3879–3907.
[16] Z. Yin, A. Prosperetti, J. Kim, Bubble growth on an impulsively powered microheater, Int. J. Heat Mass Transfer 47 (2004) 1053–1067.
[17] W.J. Yang, K. Tsutsui, Overview of boiling on microstructures-macro bubbles from micro heaters, Microscale Thermophys. Eng. 4 (2000) 7–24.
[18] Y. Hong, N. Ashgriz, J. Andrews, Experimental study of bubble dynamics on a micro heater induced by pulse heating, J. Heat Transfer 126 (2004) 259–271.
[19] M.A. Johnson, J. de la Pena, R.B. Mesler, Bubble shapes in nucleate boiling, AIChE J. 2 (1966) 344–348.
[20] J.H. Lay, V.K. Dhir, Shape of a vapor stem during nucleate boiling of saturated liquids, J. Heat Transfer 117 (1995) 394–401.
[21] Y. Chen, M. Groll, R. Mertz, R. Kulenovic, Study of forces acting on a growing bubble from smooth and enhanced tubes, Int. J. Heat Technol. 20 (2002) 31–40.
[22] P. Deng, Y.-K. Lee, P. Cheng, The growth and collapse of a micro-bubble under pulse heating, Int. J. Heat Mass Transfer 46 (2003) 4041–4050.
[23] P. Deng, Y.-K. Lee, P. Cheng, Design and characterization of a micro single bubble actuator, in: The 12th International Conference on Solid-State Sensors, Actuators and Microsystems (Transducers'03), June 8–12, Boston, 2003, pp. 647–650.
[24] P. Deng, Y.-K. Lee, P. Cheng, Characterization of an integrated self-sensing submicron bubble actuator, in: Asia-Pacific Conference of Transducers and Micro-Nano Technology (APCOT) July 4–7, Sapporo, Japan, 2004, pp. 310–315.
[25] P. Deng, Y.-K. Lee, P. Cheng, Micro bubble dynamics in DNA solutions, J. Micromech. Microeng. 14 (2004) 693–701.
[26] P. Deng, Y.-K. Lee, P. Cheng, Measurements of micro bubble nucleation temperature in DNA solutions, J. Micromech. Microeng. 15 (2005) 564–574.
[27] P. Deng, Y.-K. Lee, P. Cheng, Viscosity effects on micro bubble actuator in ssDNA solutions, in: 17th IEEE International Conference on Micro Electro Mechanical Systems, MEMS 2004, The Netherlands, 2004, pp. 25–29.
[28] B.B. Mikic, W.M. Rohsenow, P. Griffith, On bubble growth rates, Int. J. Heat Mass Transfer 13 (1970) 657–666.
[29] A. Asai, Bubble dynamics in boiling under high heat flux pulse heating, J. Heat Transfer 113 (1991) 973–979.
[30] M. Plesset, A. Prosperetti, Bubble dynamics and cavitation, Ann. Rev. Fluid Mech. 9 (1977) 145–185.